

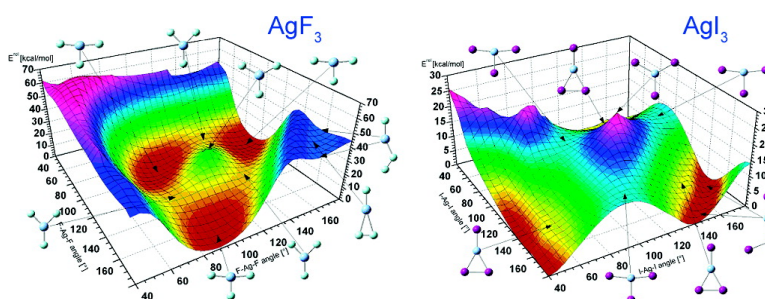
Article

## Structure and Bonding in Silver Halides. A Quantum Chemical Study of the Monomers: $\text{AgX}$ , $\text{AgX}_2$ , $\text{AgX}_3$ , and $\text{AgX}_4$ ( $\text{X} = \text{F}, \text{Cl}, \text{Br}, \text{I}$ )

Hans-Christian Mller-Rsing, Axel Schulz, and Magdolna Hargittai

*J. Am. Chem. Soc.*, **2005**, 127 (22), 8133-8145 • DOI: 10.1021/ja051442j • Publication Date (Web): 14 May 2005

Downloaded from <http://pubs.acs.org> on March 25, 2009



### More About This Article

Additional resources and features associated with this article are available within the HTML version:

- Supporting Information
- Links to the 6 articles that cite this article, as of the time of this article download
- Access to high resolution figures
- Links to articles and content related to this article
- Copyright permission to reproduce figures and/or text from this article

[View the Full Text HTML](#)

## Structure and Bonding in Silver Halides. A Quantum Chemical Study of the Monomers: $\text{Ag}_2\text{X}$ , $\text{AgX}$ , $\text{AgX}_2$ , and $\text{AgX}_3$ ( $\text{X} = \text{F}, \text{Cl}, \text{Br}, \text{I}$ )

Hans-Christian Müller-Rösing,<sup>†</sup> Axel Schulz,<sup>\*,†</sup> and Magdolna Hargittai<sup>\*,†</sup>

Contribution from the Department of Chemistry and Biochemistry, Ludwig-Maximilians University, Munich, Butenandtstrasse 5-13 (Haus D), D-81377 Munich, Germany, and the Structural Chemistry Research Group of the Hungarian Academy of Sciences, Eötvös University, Pf. 32, H-1518 Budapest, Hungary

Received March 7, 2005; E-mail: hargitta@chem.elte.hu; lex@cup.uni-muenchen.de

**Abstract:** The molecular structure of all silver halide monomers,  $\text{Ag}_2\text{X}$ ,  $\text{AgX}$ ,  $\text{AgX}_2$ , and  $\text{AgX}_3$ , ( $\text{X} = \text{F}, \text{Cl}, \text{Br}, \text{I}$ ), have been calculated at the B3LYP, MP2, and CCSD(T) levels of theory by using quasirelativistic pseudopotentials for all atoms except fluorine and chlorine. All silver monohalides are stable molecules, while the relative stabilities of the subhalides, dihalides, and trihalides considerably decrease toward the larger halogens. The ground-state structure of all  $\text{Ag}_2\text{X}$  silver subhalides has  $\text{C}_{2v}$  symmetry, and the molecules can be best described as  $[\text{Ag}_2]^+\text{X}^-$ . Silver dihalides are linear molecules;  $\text{AgF}_2$  has a  ${}^2\Sigma_g$  ground state, while all of the other silver dihalides have a ground state of  ${}^2\Pi_g$  symmetry. The potential energy surface (PES) of all silver trihalides has been investigated. Neither of these molecules has a  $D_{3h}$  symmetric trigonal planar geometry, due to their Jahn–Teller distortion. The minimum energy structure of  $\text{AgF}_3$  is a T-shaped structure with  $\text{C}_{2v}$  symmetry. For  $\text{AgCl}_3$ ,  $\text{AgBr}_3$ , and  $\text{AgI}_3$ , the global minimum is an L-shaped structure, which lies outside the Jahn–Teller PES. This structure can be considered as a donor–acceptor system, with  $\text{X}_2$  acting as donor and  $\text{AgX}$  as acceptor. Thus, except for  $\text{AgF}_3$ , in the other three silver trihalides, silver is not present in the formal oxidation state 3.

### Introduction

The halides of group 11 metals (sometimes also called coinage metals) have attracted much interest recently, both by experiments and computations. One reason is the many practical applications, such as the use of silver(I) halides in photography<sup>1,2</sup> and holography,<sup>3</sup> the use of copper(II) halides as catalysts<sup>4</sup> and of  $\text{CuCl}_2$  as a possible chemical laser,<sup>5</sup> and the new interest in gold halides, some of which appears to have rather unexpected structures.<sup>6</sup>  $\text{AgF}_2$  and especially  $\text{AgF}_3$  are among the strongest oxidizing agents known today.<sup>7–9</sup> The unique silver subfluoride,  $\text{Ag}_2\text{F}$ , is a metallic conductor<sup>10</sup> and superconductor.<sup>11</sup> Intermediate valence  $\text{Ag(II)/Ag(III)}$  fluorides have been studied as potential superconductors by Grochala and Hoffmann, who also

give a detailed summary of the literature on higher-valence silver fluorides.<sup>12</sup> Due to their technological importance in photography, silver(I) chloride and bromide have been studied extensively both in the solid and in the liquid phase.<sup>13</sup> It was discovered as early as 1879, based on vapor pressure measurements,<sup>14</sup> that the vapors of copper halides contain small clusters. These clusters<sup>15–20</sup> as well as those of silver(I) halides<sup>20</sup> have been the subject of different experimental and, recently, more and more computational studies.<sup>21–23</sup>

The reasons for the theoretical interest in group 11 halides are manifold. They are ideal for studying relativistic effects on

<sup>†</sup> Ludwig-Maximilians University.

<sup>‡</sup> Eötvös University.

- (1) Greenwood, N. N.; Eamshaw, A. *Chemistry of the Elements*; Pergamon Press: Oxford, 1984; p 1376.
- (2) Shalabi, A. S. *J. Comput. Chem.* **2002**, *23*, 1104.
- (3) (a) Neipp, C.; Pascual, C.; Belendez, A. *J. Phys. D: Appl. Phys.* **2002**, *35*, 957. (b) Blyth, J.; Millington, R. B.; Mayes, A. G.; Lowe, C. R. *Imaging Sci. J.* **1999**, *47*, 87.
- (4) Kang, S. K.; Yoon, S. K.; Kim, Y. M. *Org. Lett.* **2001**, *3*, 2697.
- (5) Ramirez-Solis, A.; Daudey, J. P. *J. Chem. Phys.* **2004**, *120*, 3221.
- (6) Schulz, A.; Hargittai, M. *Chem.—Eur. J.* **2001**, *7*, 3657.
- (7) Hoffmann, R. *Am. Sci.* **2001**, *89*, 311.
- (8) Zemva, B.; Lutar, K.; Jeshi, A.; Casteel, W. J.; Wilkonson, A. P.; Cox, D. E.; Von Dreese, R. B.; Bormann, H.; Bartlett, N. *J. Am. Chem. Soc.* **1991**, *113*, 4192.
- (9) Hargittai, I. *Chem. Intell.* **2000**, *6*, 7.
- (10) Ido, S.; Uchida, S.; Kitazawa, K.; Tanaka, S. *J. Phys. Soc. Jpn.* **1988**, *57*, 997.
- (11) Andres, K.; Kuebler, N. A.; Robin, M. B. *J. Phys. Chem. Solids* **1966**, *27*, 1747.

- (12) Grochala, W.; Hoffmann, R. *Angew. Chem., Int. Ed.* **2001**, *40*, 2742.
- (13) For example, see: (a) Bogels, G.; Meekes, H.; Bennema, P.; Bollen, D. *Imaging Sci. J.* **2001**, *49*, 33. (b) Mitev, P. D.; Saito, M.; Waseda, Y. *Mater. Trans.* **2001**, *42*, 829. (c) Di Cicco, A.; Taglienti, M.; Minicucci, M.; Filippini, A. *Phys. Rev. B* **2000**, *62*, 12001.
- (14) Meyer, V.; Meyer, C. *Berichte* **1879**, *12*, 1112.
- (15) (a) Guido, M.; Gigli, G.; Balducci, G. *J. Chem. Phys.* **1972**, *57*, 3731. (b) Guido, M.; Balducci, G.; Gigli, G.; Spoliti, M. *J. Chem. Phys.* **1971**, *55*, 4566.
- (16) Wong, C.-H.; Schomaker, V. *J. Phys. Chem.* **1957**, *61*, 358.
- (17) Butaev, B. S.; Gershikov, A. G.; Spiridonov, V. P. *Vestn. Mosk. Univ. Ser. Khim.* **1978**, *19*, 734.
- (18) Krabbes, v. G.; Oppermann, H. *Z. Anorg. Allg. Chem.* **1977**, *435*, 33.
- (19) Hargittai, M.; Schwerdtfeger, P.; Reffy, B.; Brown, R. *Chem.—Eur. J.* **2003**, *9*, 327.
- (20) Martin, T. P.; Schaber, H. *J. Chem. Phys.* **1980**, *73*, 3541.
- (21) (a) Rabilloud, F.; Spiegelmann, F.; Heully, J. L. *J. Chem. Phys.* **1999**, *111*, 8925. (b) Rabilloud, F.; Spiegelmann, F.; L'Hermite, J. M.; Labastie, P. *J. Chem. Phys.* **2001**, *114*, 289.
- (22) Zhang, H.; Schelly, Z. A.; Marynick, D. S. *J. Phys. Chem. A* **2000**, *104*, 6287.
- (23) Schwerdtfeger, P.; Krawczyk, R. P.; Hammerl, A.; Brown, R. *Inorg. Chem.* **2004**, *43*, 6707.

the molecular properties in a series of molecules, as the gold monohalides are probably the ultimate examples of relativistic effects on structural parameters due to the relativistic contraction reaching a maximum with the filled 5d shell of gold.<sup>24,25</sup> The relativistic effect in gold monohalides has been extensively studied.<sup>24,26</sup> Closed-shell interactions, among them the  $d^{10}\cdots d^{10}$  interaction, for which the monohalides of the coinage metals are typical examples, have also received considerable interest.<sup>27,28</sup> Advances in computational power and sophistication of computer programs have made these systems available for high-quality computations. A recent study using new spin-orbit pseudopotentials for the coinage metals determined the spectroscopic properties of all their monohalides, except their iodides.<sup>29</sup> It also gave references to the experimental and some earlier computational studies of these monohalides. The new computations also bring up the question of the relative importance of correlation and relativistic effects on molecular parameters.<sup>30</sup>

Another topic in connection with the halides of group 11 metals is the Jahn–Teller (JT) effect.<sup>31</sup> It has been shown by experimental<sup>32</sup> as well as computational studies<sup>6,32–34</sup> that the lighter halide gold trihalides are typical Jahn–Teller systems in that they have a distorted T- or Y-shaped structure rather than the usual  $D_{3h}$  symmetric trigonal planar structure. The global minimum structure of gold triiodide lies outside the JT surface, and the molecule has an L-shaped structure that can be considered as a donor–acceptor molecule between AuI and  $I_2$ .<sup>6</sup>

The spectroscopic parameters of all monomeric silver monohalides have been measured (AgF,<sup>35</sup> AgCl,<sup>36</sup> AgBr,<sup>37</sup> and AgI<sup>37</sup>), but no geometrical parameters have been determined experimentally for any other silver halide molecule. Computational studies have been performed on silver halides, especially on the bromides, due to their importance in the imaging industry. All of the monomeric monohalides have been studied at different levels of sophistication (see refs 29 and 38 and references therein). Several neutral clusters of silver bromide have also been studied,<sup>21,22</sup> and some of the results will be discussed later.<sup>39</sup> Silver dibromide and silver subbromide were also studied by Rabilloud et al.,<sup>21</sup> but none of the other silver dihalides and subhalides have been investigated yet, neither have the possible trihalides and the dimers and larger oligomers of the other silver monohalides and the dimers of the trihalides. We decided to

fill this gap and calculate the structure of all silver sub-, mono-, di-, and trihalide monomers (this paper), and the dimers, trimers, and tetramers of silver monohalides and the dimers of silver trihalides.<sup>39</sup> Even though some computational results for the silver monohalides have been communicated, we found it important to get a consistent picture on *all* silver halides with the same method and basis set; this enhances the reliability of the trends observed for a series of molecules. A further goal of our study is to compare the structures, stabilities, and other properties of silver and gold halides, based on our previous paper describing the structure of neutral gold halides, AuX and AuX<sub>3</sub>, and their dimers.<sup>6</sup>

## Computational Details

The calculations were carried out with the Gaussian98 program package.<sup>40</sup> The data analyses were performed with Molden version 3.6<sup>41</sup> and GaussView 2.08.<sup>42</sup> Different basis sets have been checked. For the silver atom, a multielectron-adjusted quasirelativistic effective core potential (ECP) covering 28 electrons ([Ar]3d<sup>10</sup>) and two different associated basis sets were used: a smaller one, (8s7p6d)/[6s5p3d]-GTO valence basis set (termed “SB”), and a larger one, (8s7p6d2f1g)/[6s5p3d2f1g] (termed “LB”). For fluorine and chlorine, all electron basis sets were applied, again, a smaller one, 6-31G(d) “SB”, and a larger one, 6-311+G(3df) “LB”. For bromine and iodine, quasirelativistic effective core potentials were used, an ECP covering 28 electrons ([Ar]3d<sup>10</sup>) for bromine and an ECP covering 46 electrons ([Kr]4d<sup>10</sup>) for iodine, with two associated basis sets: a smaller one, (5s5p1d)/[3s3p1d] “SB”, and a larger one, (14s10p3d2f1g)/[4s4p3d2f1g] “LB”. Both the pseudopotentials and the corresponding basis sets were those of the Stuttgart group.<sup>43</sup>

Three different methods were used, a density functional with the B3LYP formalism,<sup>44</sup> MP2, and the CCSD(T) method. Full geometry optimizations were carried out for all molecules by all three methods, each with both types of basis sets (SB and LB). For the Ag<sub>2</sub>X and AgX<sub>3</sub> molecules, different possible geometrical arrangements were considered and for the AgX<sub>2</sub> molecules, two different electronic states. The molecular models and numbering of atoms for the computed structures are shown in Figure 1. The relative energies, as well as the energies of certain decomposition reactions, are given in the Supporting Information. Frequency analyses were carried out for each of the possible arrangements of all molecules; the frequencies for all species are given in the Supporting Information.

Comparison of our computed parameters with the available experimental data (see Supporting Information for details of the comparison) suggested that the CCSD(T) method with the large basis set (LB) gives the best agreement; therefore, this set of data will be communicated in the paper. The results of the other computations are given in the Supporting Information.

To check the possible Jahn–Teller distortion of silver trihalides, we have calculated their PES at the B3LYP level. For each molecule, the energy was calculated as a function of the two X–Ag–X angles in 5° steps (for definition of these angles, see Figure 1). None of the determined points have been corrected for zero-point vibrations; such

- (24) Pyykkö, P. *Chem. Rev.* **1988**, *88*, 563.  
 (25) Pyykkö, P. *Angew. Chem., Int. Ed.* **2004**, *43*, 4412.  
 (26) (a) Schwerdtfeger, P.; Dolg, M.; Schwarz, W. H. E.; Bowmaker, G. A.; Boyd, P. D. W. *J. Chem. Phys.* **1989**, *91*, 1762. (b) Schwerdtfeger, P. *Mol. Phys.* **1995**, *86*, 359. (c) Schwerdtfeger, P.; McFeaters, J. S.; Liddell, M. J.; Hrusak, J.; Schwarz, H. *J. Chem. Phys.* **1995**, *103*, 245.  
 (27) Pyykkö, P. *Chem. Rev.* **1997**, *97*, 597.  
 (28) Desiraju, G. J. *Chem. Soc., Dalton Trans.* **2000**, 3745.  
 (29) Guichemerre, M.; Chambaud, G.; Stoll, H. *Chem. Phys.* **2002**, *280*, 71.  
 (30) Ilias, M.; Furdik, P.; Urban, M. *J. Phys. Chem. A* **1998**, *102*, 5263.  
 (31) Jahn, H. A.; Teller, E. *Proc. R. Soc., London, Ser. A* **1937**, *161*, 220.  
 (32) Réffy, B.; Kolonits, M.; Schulz, A.; Klapötke, T. M.; Hargittai, M. *J. Am. Chem. Soc.* **2000**, *122*, 3127.  
 (33) Hargittai, M.; Schulz, A.; Réffy, B.; Kolonits, M. *J. Am. Chem. Soc.* **2001**, *123*, 1449.  
 (34) Schwerdtfeger, P.; Boyd, P. D. W.; Brienne, S.; Burrell, A. K. *Inorg. Chem.* **1992**, *31*, 3411.  
 (35) (a) Hoefl, J.; Lovas, F. J.; Tiemann, E.; Topping, T. *Z. Naturforsch.* **1970**, *25a*, 35. (b) Barrow, R. F.; Clement, R. M. *Proc. R. Soc.* **1971**, *A322*, 243.  
 (36) (a) Pearson, E. F.; Gordy, W. *Phys. Rev.* **1966**, *152*, 42. (b) Krisher, L. C.; Norris, W. G. *J. Chem. Phys.* **1966**, *44*, 391.  
 (37) (a) Hoefl, J.; Lovas, F. J.; Tiemann, E.; Topping, T. *Z. Naturforsch.* **1971**, *26a*, 240. (b) Krisher, L. C.; Norris, W. G. *J. Chem. Phys.* **1966**, *44*, 974.  
 (38) Hargittai, M. *Chem. Rev.* **2000**, *100*, 2233.  
 (39) Müller-Rösing, H.-C.; Schulz, A.; Hargittai, M. In preparation.

- (40) Frisch, M. J. et al. *Gaussian 98*, revision A.6; Gaussian Inc.: Pittsburgh, PA, 1998.  
 (41) *Molden*, version 3.6; Gijs Schaftenaar: Nijmegen, The Netherlands, 1991.  
 (42) *GaussView*, version 2.08; Semichem, Inc./Gaussian, Inc.: Pittsburgh, PA, 1998.  
 (43) (a) Andrae, D.; Häussermann, U.; Dolg, M.; Stoll, H.; Preuss, H. *Theor. Chim. Acta* **1990**, *77*, 123. (b) Dolg, M. Effective Core Potentials. In *Modern Methods and Algorithms of Quantum Chemistry*, Band 3, Proceedings 2, Auflage; Grotendorst, J., Ed.; John von Neumann Institute for Computing, Jülich, NIC Series, 2000; pp 507–540.  
 (44) (a) Bauschlicher, C. W.; Partridge, H. *Chem. Phys. Lett.* **1994**, *231*, 277. (b) Becke, A. D. *J. Chem. Phys.* **1993**, *98*, 5648. (c) Becke, A. D. *Phys. Rev. A* **1988**, *38*, 3098. (d) Lee, C.; Yang, W.; Parr, R. G. *Phys. Rev. B* **1988**, *37*, 785. (e) Vosko, S. H.; Wilk, L.; Nusair, M. *Can. J. Phys.* **1980**, *58*, 1200.

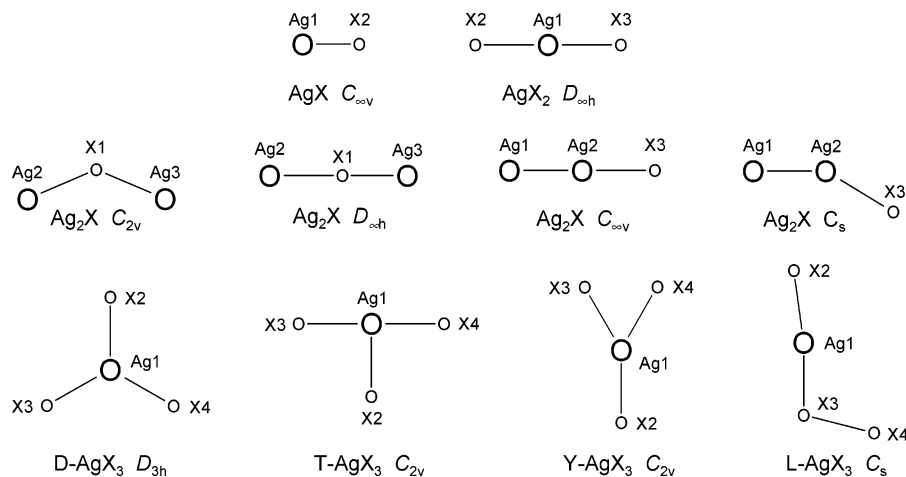


**Figure 1.** Molecular models of different silver halides. The numbering of atoms is also given.

corrections are calculated to be rather small, of the order of 0.1–0.2 kcal/mol, in the harmonic approximation.

The B3LYP density functional method was used for bonding, MO, and population analysis (single-point calculations utilizing the best CCSD(T) geometry). NBO analyses were performed with the NBO program version 3.1,<sup>45</sup> implemented in Gaussian98. Our test calculations showed that the calculated partial charges depended on whether we used all electron bases or ECPs; therefore, for consistency, Stuttgart-type ECPs<sup>43</sup> were used for all halogens in these calculations, at the CCSD(T)/all electron geometry. The so-called Wiberg bond indices were also calculated for all molecules; they describe the classical bond orders in molecules (for the definition of Wiberg indices, see Supporting Information).<sup>46</sup>

Bader's Atoms in Molecules (AIM)<sup>47</sup> method was used to analyze the chemical bonding in all molecules. AIM analyses were carried out with all-electron basis sets (Ag: (17s12p8d)/[6s4p3d];<sup>48</sup> F, Cl, Br: 6-311+G(3df); and I: (19s15p9d)/[8s7p5d]). For more details, see the Supporting Information.

## Results and Discussion

**Silver Subhalides.** From the  $\text{Ag}_2\text{X}$  molecules, only  $\text{Ag}_2\text{F}$  is known experimentally and it is unique in being the only metal subfluoride known. It has a layer structure in the crystal,<sup>49</sup> in which there are double  $[\text{AgAg}]^+$  layers connected with van der Waals interactions and separated by layers of fluoride ions. This makes it possible to use it as a metallic conductor or superconductor, as mentioned in the Introduction. The  $\text{Ag}\cdots\text{Ag}$  distance within the layers is 2.996 Å (compare with the 2.89 Å distance in the silver metal), while the distance between Ag atoms in neighboring layers is 3.4 Å.<sup>49</sup>

There are several possible structures for the isolated molecules of  $\text{Ag}_2\text{X}$ , as shown in Figure 1. Each of them has been checked by the computations, and their geometrical parameters are given

in Table 1. According to all calculations, the global minimum structure ( ${}^2\text{A}_1$ ) has  $\text{C}_{2v}$  symmetry with the halogen as the central atom (see Figure 1). As to the other isomers, the three different computational methods give somewhat different results. There is another  $\text{Ag}-\text{F}-\text{Ag}$  arrangement ( ${}^2\Sigma_g$ ) with  $\text{D}_{\infty h}$  symmetry, and it seems to be the one with the highest energy by all methods. The energy difference between this structure and the  $\text{C}_{2v}$  symmetry structure is about 14 kcal/mol by the MP2 and CCSD(T) methods for the chlorides, bromides, and iodides, and a few kcal/mol smaller for the fluorides. The density functional calculations underestimate this energy difference by about 50%. Another important disagreement between the different methods is that while the CCSD(T) method finds the  $\text{D}_{\infty h}$  structure a true minimum, the B3LYP calculation does that only for the  $\text{Ag}_2\text{F}$  and  $\text{Ag}_2\text{Cl}$  molecules, and for the bromide and iodide, this structure is only a second-order saddle point with two imaginary frequencies.

There are two more possible structures for the  $\text{Ag}_2\text{X}$  molecules, having direct  $\text{Ag}-\text{Ag}$  bonds, one linear ( $\text{C}_{\infty v}$ ) and another bent ( $\text{C}_s$ ), as shown in Figure 1. According to both the CCSD(T) and the MP2 methods, the  $\text{C}_s$  symmetry structures are unstable and they optimize to the linear  $\text{C}_{\infty v}$  symmetry structures, which, according to the frequency analyses, are stable minima with about 4–6 kcal/mol higher energies than those of the  $\text{C}_{2v}$  global minimum structures. The B3LYP method, again, paints a different picture. Contrary to the other methods, it finds the  $\text{C}_s$  structures to be stable minima and the  $\text{C}_{\infty v}$  structures as second-order saddle points for all halides except the fluoride, for which that structure is also a minimum.

There are several possible explanations why such differences occur between the results of different methods. The lowest frequencies, especially for the higher-energy structures, are very low, indeed, below  $50\text{ cm}^{-1}$ . The energy differences are also very small between some of these species, and for the problematic  $\text{C}_{\infty v}-\text{C}_s$  isomers, they are sometimes less than 1 kcal/mol. Thus, the result of computations may be rather uncertain, depending on the method and basis set. It is to be noted that the use of different basis sets influences only the energies of the structures but not their apparent stability. Our further discussion of the different isomers of  $\text{Ag}_2\text{X}$  molecules is based on the CCSD(T) calculations. The relative energies of the different  $\text{Ag}_2\text{X}$  isomers (CCSD(T)/LB) are shown in

- (45) (a) Glendening, E. D.; Reed, A. E.; Carpenter, J. E.; Weinhold, F. *NBO, version 3.1*. (b) Carpenter, J. E.; Weinhold, F. *J. Mol. Struct. (THEOCHEM)* **1988**, *169*, 41. (c) Foster, J. P.; Weinhold, F. *J. Am. Chem. Soc.* **1980**, *102*, 2, 7211. (d) Reed, A. E.; Weinhold, F. *J. Chem. Phys.* **1983**, *78*, 4066. (e) Reed, A. E.; Weinstock, R. B.; Weinhold, F. *J. Chem. Phys.* **1985**, *83*, 735. (f) Reed, A. E.; Curtiss, L. A.; Weinhold, F. *Chem. Rev.* **1988**, *88*, 899. (g) Reed, A. E.; Schleyer, P. v. R. *J. Am. Chem. Soc.* **1987**, *109*, 7362. (h) Reed, A. E.; Schleyer, P. v. R. *Inorg. Chem.* **1988**, *27*, 3969. (i) Weinhold, F.; Carpenter, J. E. *The Structure of Small Molecules and Ions*; Plenum Press: New York, 1988; p 227.
- (46) Wiberg, K. *Tetrahedron* **1968**, *24*, 1083.
- (47) Bader, R. F. W. *Atoms in Molecules: A Quantum Theory*; The International Series of Monographs of Chemistry, Oxford University Press: Oxford, 1990.
- (48) Ahlrichs, R.; May, K. *Phys. Chem. Chem. Phys.* **2000**, *2*, 943–945.
- (49) Williams, A. J. *Phys. Condens. Matter* **1989**, *1*, 2569.



**Table 1.** Computed Geometrical Parameters of Silver Halide Molecules,  $\text{Ag}_2\text{X}$ ,  $\text{AgX}_2$ , and  $\text{AgX}_3$  ( $\text{X} = \text{F}, \text{Cl}, \text{Br}, \text{I}$ ) at the CCSD(T)/LB Level (Distances in Angstrom, Angles in Degrees)<sup>a</sup>

			F	Cl	Br	I
$\text{Ag}_2\text{X}$	$\text{Ag}_2\text{X}, {}^2\text{A}_1, \text{C}_{2v}$	Ag–X	2.188	2.517	2.599	2.765
		$\angle\text{Ag–X–Ag}$	75.5	63.9	61.6	57.4
	$\text{Ag}_2\text{X}, {}^2\Sigma_g^+, \text{D}_{\infty h}$	Ag $\cdots$ Ag	2.681	2.664	2.663	2.654
		Ag–X	2.110	2.425	2.512	2.678
$\text{AgX}_2$	$\text{Ag}_2\text{X}, {}^2\Sigma_g^+, \text{D}_{\infty h}$	Ag1–Ag2	2.682	2.682	2.690	2.694
		Ag2–X3	1.997	2.305	2.399	2.566
	$\text{AgX}_2, {}^2\Pi_g, \text{D}_{\infty h}$	Ag–X	1.891	2.253	2.375	2.586
		Ag–X	1.889	2.235	2.351	2.546
$\text{AgX}_3$	$\text{D–AgX}_3, {}^1\text{E}', \text{D}_{3h}$	Ag–X	1.909	2.268	2.383	2.583
		Ag–X <sup>b</sup>	1.902	2.304	2.442	2.659
	$\text{T–AgX}_3, {}^1\text{A}_1, \text{C}_{2v}$	Ag1–X2	1.876	2.243	2.367	2.572
		Ag1–X3	1.860	2.238	2.364	2.557
$\text{Y–AgX}_3, {}^1\text{A}_1, \text{C}_{2v}$	$\angle\text{X2–Ag1–X3}$	94.0	94.8	94.7	94.6	
	Ag1–X2	1.904	2.246			
	Ag1–X3	1.863	2.250			
	X3–X4	2.522	2.890			
$\text{L–AgX}_3, {}^1\text{A}', \text{C}_s$	$\angle\text{X2–Ag1–X3}$	137.4	140.0			
	Ag1–X2	1.979	2.312	2.379	2.562	
	Ag1–X3	2.410	2.485	2.519	2.722	
	Ag1–X4	3.075	3.776	3.691	4.022	
	X3–X4	1.419	2.086	2.304	2.576	
	$\angle\text{X2–Ag1–X3}$	176.4	170.0	177.9	177.9	
	$\angle\text{Ag1–X3–X4}$	103.9	111.1	99.8	98.8	

<sup>a</sup>LB: large basis set; see Computational Details. <sup>b</sup>CCSD(T)/SB level, SB: small basis set; see Computational Details.

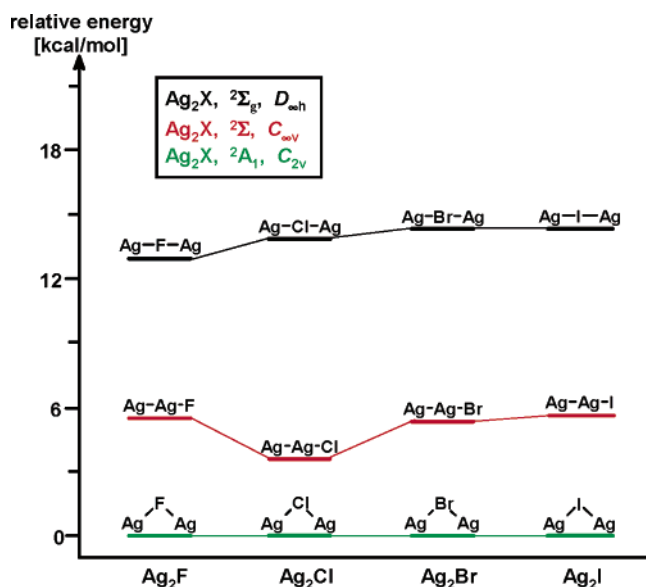
**Figure 2.** Relative energies of different  $\text{Ag}_2\text{X}$  isomers from CCSD(T)/LB calculations (LB: large basis set; see Computational Details).

Figure 2; the ones for the other methods are given in the Supporting Information.

The computed NPA partial charges for all molecules are given in Table 2 and the Wiberg indices in Table 3. The Ag–X bonds in all molecules are highly polar. In trying to understand the bonding in the silver subhalides, different Lewis representations can be suggested for them, as shown in Figure 3.

For the  $\text{C}_{2v}$  symmetry structure (Figure 3a), Lewis representations **A** and **B** represent covalent bonding between one Ag atom and the X atom and leaves the other Ag atom nonbonding, whereas structure **C** describes a single electron bond between the two Ag atoms, with a +1 overall charge and the X atom with a –1 charge. Lewis representation **C** is in agreement with the NBO partial charges. Further support for this structure is the total atomic spin densities in the different isomers of  $\text{Ag}_2\text{X}$

molecules, given in the Supporting Information. In the  $\text{C}_{2v}$  isomer of  $\text{Ag}_2\text{F}$ , the odd-electron density is almost completely localized on the  $\text{Ag}_2$  unit, in fact, between the two Ag centers, as seen from Figure 4. The Ag $\cdots$ Ag NBO occupancy in  $\text{Ag}_2\text{F}$  is about 97%.

It is worthwhile to compare the structure of the  $[\text{Ag}_2]^+$  fragment with those of the  $\text{Ag}_2$  molecule and the  $\text{Ag}_2^+$  ion. The Ag $\cdots$ Ag distance in  $\text{Ag}_2\text{F}$  is 2.681 Å, and this is about 0.04 Å shorter than the Ag–Ag bond length in the free gaseous  $\text{Ag}_2^+$  ion (2.718 Å) but much longer (by about 0.13 Å) than that in the  $\text{Ag}_2$  molecule (2.550 Å) [all distances at the CCSD(T)/LB level]. The Ag $\cdots$ Ag distance of 2.681 Å in  $\text{Ag}_2\text{F}$  is much shorter than twice the covalent radius (1.53 Å) of Ag, let alone twice its van der Waals radius (1.72 Å). Figure 5 shows one of the molecular orbitals of the  $\text{C}_{2v}$  symmetric  $\text{Ag}_2\text{X}$  halides; the direct Ag $\cdots$ Ag interaction is obvious from them. Thus, for the  $\text{C}_{2v}$  symmetric  $\text{Ag}_2\text{F}$  molecule, we have a covalently bonded  $[\text{Ag}_2]^+$  unit in Coulombic interaction with the fluoride ion. As we go from  $\text{Ag}_2\text{F}$  toward the larger halides, the Ag–X–Ag bond angles and the Ag $\cdots$ Ag distances slightly decrease, and this is the consequence of the decreasing electronegativity of the central halogen atom. The Wiberg indices (see Table 3) slightly increase toward the larger halides, and this is in agreement with the MO picture of Figure 5, as well. It is also worth mentioning that the Wiberg indices for the Ag $\cdots$ Ag interaction in the  $\text{Ag}_2\text{X}$  species are close to that in the  $\text{Ag}_2^+$  ion, indicating that it is realistic to imagine that the  $\text{Ag}_2^+$  ion is part of the  $\text{Ag}_2\text{X}$  structure. The partial charges, as well as the spin densities on the  $[\text{Ag}_2]^+$  unit, decrease in this direction, and this leads to decreasing stability.

We can also describe the bonding in the global minimum  $\text{C}_{2v}$  symmetry structure in terms of localized bonds. The Ag–X bond in these molecules can be considered a three-electron three-center bond, and as such, it is weaker than the bond in the monohalides. Accordingly, the bonds are about 0.2 Å longer than those in the  $\text{AgX}$  monohalides in all four cases; a very large difference, indeed.

**Table 2.** Results of NBO Analysis for  $\text{Ag}_2\text{X}$ ,  $\text{AgX}$ ,  $\text{AgX}_2$ ,  $\text{AgX}_3$  ( $\text{X} = \text{F}, \text{Cl}, \text{Br}, \text{I}$ ) Molecules ( $q$  in  $e$ )<sup>a</sup>

$\text{Ag}_2\text{X}$ , ${}^2A_1, C_{2v}$	$q(\text{Ag}2/3)$	$q(\text{X})$		
F	0.43632	-0.87264		
Cl	0.36948	-0.73896		
Br	0.33974	-0.67948		
I	0.29441	-0.58883		
$\text{Ag}_2\text{X}$ , ${}^2\Sigma_g, D_{\infty h}$	$q(\text{Ag}2/3)$	$q(\text{X})$		
F	0.45261	-0.90523		
Cl	0.40153	-0.80306		
Br	0.37615	-0.75230		
I	0.33348	-0.66697		
$\text{Ag}_2\text{X}$ , ${}^2\Sigma, C_{\infty v}$	$q(\text{Ag}1)$	$q(\text{Ag}2)$	$q(\text{X})$	
F	0.20203	0.62667	-0.82870	
Cl	0.21127	0.49818	-0.70945	
Br	0.20994	0.44086	-0.65080	
I	0.20566	0.35031	-0.55597	
$\text{AgX}$	$q(\text{Ag})$	$q(\text{X})$		
F	0.81867	-0.81867		
Cl	0.70736	-0.70736		
Br	0.65479	-0.65479		
I	0.57155	-0.57155		
$\text{AgX}_2$ , ${}^2\Sigma_g, D_{\infty h}$	$q(\text{Ag})$	$q(\text{X}2/3)$		
F	1.34810	-0.67405		
Cl	1.08837	-0.54418		
Br	0.99718	-0.49859		
I	0.86567	-0.43283		
$\text{AgX}_2$ , ${}^2\Pi_g, D_{\infty h}$	$q(\text{Ag})$	$q(\text{X}2/3)$		
F	1.11887	-0.55944		
Cl	0.77339	-0.38670		
Br	0.66806	-0.33403		
I	0.53135	-0.26568		
T- $\text{AgX}_3$	$q(\text{Ag})$	$q(\text{X}2)$	$q(\text{X}3/4)$	
F	1.56437	-0.44700	-0.55868	
Cl	1.02817	-0.23535	-0.39641	
Br	0.87337	-0.18266	-0.34536	
I	0.66909	-0.12073	-0.27418	
L- $\text{AgX}_3$	$q(\text{Ag})$	$q(\text{X}2)$	$q(\text{X}3)$	$q(\text{X}4)$
F	0.82800	-0.79300	-0.04300	0.00800
Cl	0.65064	-0.68878	0.00051	0.03763
Br	0.58620	-0.63527	0.01399	0.03508
I	0.48939	-0.56327	0.03697	0.03690

<sup>a</sup> B3LYP/SB calculation at the CCSD(T)/LB geometries using ECPs for all atoms; see Computational Details.

Energetically, the next stable structure is the one with  $C_{\infty v}$  symmetry. It has a rather short Ag–X bond, about 0.2 Å shorter than the Ag–X bond in the  $C_{2v}$  isomer and only about 0.01 Å longer than the bond in the monohalides. The Ag1–Ag2 bond is about 0.02–0.04 Å longer than the  $\text{Ag}\cdots\text{Ag}$  distance in the  $C_{2v}$  isomer, except for  $\text{Ag}_2\text{F}$ , where the two are about the same. According to the NBO analysis, there is a rather large positive partial charge (0.6e) on the Ag2 atom (the one connected to the halogen) in  $\text{Ag}_2\text{F}$ , and a much smaller one (0.2e) on Ag1 (the AIM partial charge on the Ag1 atom is about the same, while on Ag2, it is only about 0.45e). At the same time, the spin density of Ag1 (the one not connected to the halogen) is about twice as large as that of Ag2 (in the fluorine derivative). This suggests that in the Lewis representations of this isomer (see Figure 3b), structures **B** and **C** are better descriptions than structure **A**.

The  $D_{\infty h}$  symmetry structure is the highest in energy, although according to the CCSD(T) computations, it is a stable structure.

**Table 3.** Wiberg Bond Indices for All Silver Halides<sup>a</sup>

	Ag–Ag	Ag–X	X–X
$\text{Ag}_2$	1.0086		
$\text{Ag}_2^+$	0.2899		
$\text{X}_2$			
		F	1.0033
		Cl	1.0264
		Br	1.0238
		I	1.0212
$\text{Ag}_2\text{X}$ , ${}^2A_1, C_{2v}$		F	0.3100
		Cl	0.3413
		Br	0.3519
		I	0.3667
$\text{Ag}_2\text{X}$ , ${}^2\Sigma_g, D_{\infty h}$		F	0.2093
		Cl	0.1845
		Br	0.1705
		I	0.1471
$\text{Ag}_2\text{X}$ , ${}^2\Sigma, C_{\infty v}$		F	0.2038
		Cl	0.2097
		Br	0.2172
		I	0.2331
$\text{AgX}$		F	0.3552
		Cl	0.5264
		Br	0.5981
		I	0.7007
$\text{AgX}_2$ , ${}^2\Sigma_g, D_{\infty h}$		F	0.2892
		Cl	0.3314
		Br	0.3281
		I	0.3150
$\text{AgX}_2$ , ${}^2\Pi_g, D_{\infty h}$		F	0.3737
		Cl	0.4396
		Br	0.4454
		I	0.4586
T- $\text{AgX}_3$		F (X2)	0.5643
		F (X3/4)	0.4217
		Cl (X2)	0.5601
		Cl (X3/4)	0.4434
		Br (X2)	0.5245
		Br (X3/4)	0.4407
		I (X2)	0.4610
		I (X3/4)	0.4400
L- $\text{AgX}_3$		F (X2)	0.3431
		F (X3)	0.0714
		F (X4)	0.0335
		Cl (X2)	0.4912
		Cl (X3)	0.1774
		Cl (X4)	0.0289
		Br (X2)	0.5331
		Br (X3)	0.2215
		Br (X4)	0.0320
		I (X2)	0.5876
		I (X3)	0.2621
		I (X4)	0.0265

<sup>a</sup> B3LYP/SB level at the CCSD(T)/LB geometries.

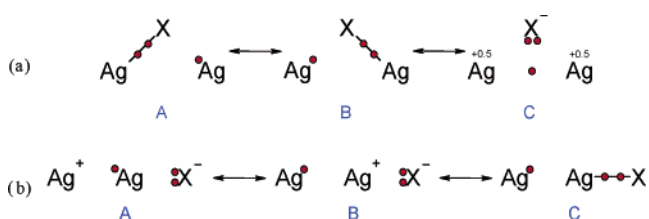


**Figure 3.** Different Lewis representations of  $\text{Ag}_2\text{X}$  subhalides (a) for  $C_{2v}$  symmetry and (b) for  $C_{\infty v}$  symmetry.

The partial charges in this molecule are about as large as those in the  $C_{2v}$  structure. Interestingly, in the  $D_{\infty h}$  structures, the Ag–X bonds are shorter, by about 0.09 Å than in the more stable  $C_{2v}$  symmetry structures. A possible reason is that in the  $C_{2v}$  structures, the odd electron density is localized between the two Ag atoms, and this may cause a repulsive effect toward the halogen ion, resulting in a longer Ag–X bond length.

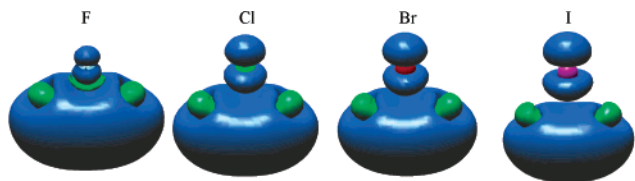


**Figure 4.** Plots of the spin density for the ground state ( $C_{2v}$  symmetry)  $Ag_2X$  molecules (HF densities at the CCSD(T)/LB geometries).

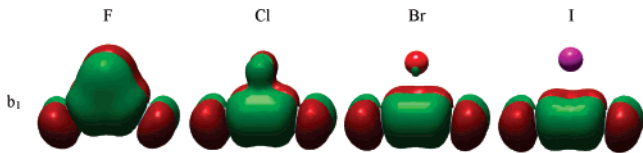


**Figure 5.**  $\pi$ -type molecular orbitals of the ground state ( $C_{2v}$  symmetry)  $Ag_2X$  molecules (HF orbitals at CCSD(T)/LB geometries).

The reason for the overall stability of the  $C_{2v}$  isomers is, first, the stabilizing effect of the direct  $Ag\cdots Ag$  interaction, which is enforced by the favorable electrostatic interaction between the  $[Ag_2]^+$  and the  $X^-$  ions. In the  $D_{\infty h}$  structure, the direct  $Ag\cdots Ag$  interaction is missing, while in the  $C_{\infty v}$  arrangement, the stabilizing effect of the direct  $Ag\cdots Ag$  interaction is lost due to the asymmetry of the structure.

There has only been one other computational study on an  $Ag_2X$  molecule, namely, of  $Ag_2Br$  by Rabilloud et al.<sup>21</sup> Only the  $C_{2v}$  symmetry structure was studied, and their MRPT2 results ( $Ag-Br$  2.646 Å and  $Ag-Br-Ag$  61°) are in agreement with ours (see Table 1).

**Silver Monohalides.** All four monohalides of silver are well-known compounds with many practical applications (vide supra). The first three monohalides are rock-salt-type crystals, while  $AgI$  has a wurtzite-type crystal structure that transforms into another one with high ionic conductivity at high temperatures.<sup>50</sup> The bond lengths of the free monomeric molecules have been determined by microwave spectroscopy.<sup>35–37</sup> Comparison of our computed bond lengths (see Table 4) with the experimental ones shows good agreement for all method/basis set combinations, well within 0.01 Å (except for  $AgCl$ , for which the difference is 0.016 Å). Our computed bond lengths show better agreement with the experimental values than any of the previous computations, some of which are also presented in Table 4. Our CCSD(T)/LB bond length of  $AgF$  is only 0.005 Å larger than the experimental one of 1.98318 Å from microwave spectroscopy.<sup>35</sup>

The unscaled computed harmonic frequencies (see Supporting Information) also agree well with the experimental ones; the agreement is within 8  $cm^{-1}$  for  $AgF$  and  $AgCl$ , and they are practically the same (within 1  $cm^{-1}$ ) as the experimental ones for  $AgBr$  and  $AgI$ . Some of the other computational results are also shown in Table S15.

All silver–halogen bonds are longer, on average by about 0.04 Å, than the bonds of the corresponding gold monohalides at the same computational level, CCSD(T)/SB. This is contrary to the generally observed lengthening of bonds down the groups in the periodic table. This is the result of relativistic effects that reach their maximum for gold.<sup>24</sup> According to a recent direct relativistic study of the coinage metal fluorides, the shortening of the metal halogen bond due to relativistic effects is about 0.20 Å for  $AuF$  and only 0.05 Å for  $AgF$ . Similarly, the change

in vibrational frequencies due to relativity is about 20% for  $AuF$  and only about 5% for  $AgF$ .<sup>55</sup>

**Silver Dihalides.** While the +2 oxidation state is common for copper, the first coinage metal, for silver, it appears mostly only with fluorine ligands. There are only very few chlorine and bromine systems known in which silver is in its +2 oxidation state, and there are no such iodides.<sup>12</sup> From among the pure dihalides, only  $AgF_2$  is known experimentally. For a long time, there was an uncertainty about its structure since it was assumed to be a mixed valence system,  $Ag^I[Ag^{III}F_4]$ , similarly to  $AgO$ .<sup>56</sup> It was only its neutron diffraction study that determined that silver is, indeed, in a +2 oxidation state in the crystal of  $AgF_2$ .<sup>57,58</sup> In this crystal, silver is in a tetragonally elongated octahedral coordination with four shorter and two longer  $Ag-F$  interactions, in line with the fact that for a  $d^9$  electronic configuration, a Jahn–Teller distortion of the high-symmetry octahedral coordination can be expected.

There is also a high-temperature disproportionated modification of the  $AgF_2$  crystal, with an  $Ag^I[Ag^{III}F_4]$  composition.<sup>59</sup> However, this modification is thermally unstable and undergoes an exothermic conversion to  $Ag^{II}F_2$ . Interestingly, the attempt to prepare gold difluoride,  $AuF_2$ , proved to be unsuccessful because it disproportionated.<sup>60</sup> According to Bartlett and co-workers,<sup>60</sup> this difference between  $AgF_2$  and  $AuF_2$  may be associated with the different excitation energies involved in making  $Ag(III)$  and  $Au(III)$  and also with the experience that forming metallic gold from  $Au(II)$  is more favorable than forming metallic silver from  $Ag(II)$ . According to a recent study of gold dichloride,  $AuCl_2$ , it might be stable against disproportionation in the idealized gas phase, but it very likely disproportionates in the condensed phase.<sup>61</sup>

We have calculated the gas-phase structures of silver dihalides,  $AgX_2$ . Two structures were investigated, both linear, with  $D_{\infty h}$  symmetry, one with a  $^2\Sigma_g$  and the other with a  $^2\Pi_g$  electronic state, and their geometrical parameters are given in Table 1. All methods of calculation agree that, for  $AgF_2$ , the  $^2\Sigma_g$  state is the ground state and the  $^2\Pi_g$  state is an excited state, while for all other dihalides, the order reverses. Figure 6 shows the energy differences. The CCSD(T) method predicts the energy difference between the  $^2\Sigma_g$  ground state and  $^2\Pi_g$  first excited state of  $AgF_2$  to be about 14 kcal/mol for both basis sets. For the larger halides, the  $^2\Pi_g$  state is more stable than the  $^2\Sigma_g$  state by about 4, 10, and 18 kcal/mol for the chlorides, bromides, and iodides, respectively, again at the CCSD(T) level. MP2 and B3LYP computations give somewhat different results (all the relative energies are given in the Supporting Information). We have to emphasize that these values are strongly method- and basis set-dependent, and as the experience with

(51) van Wüllen, C. *J. Chem. Phys.* **1998**, *109*, 392.

(52) Ramirez-Solis, A.; Daudey, J. P. *J. Chem. Phys.* **2000**, *113*, 8580.

(53) Ramirez-Solis, A. *J. Chem. Phys.* **2002**, *117*, 1047.

(54) Ramirez-Solis, A. *J. Chem. Phys.* **2003**, *118*, 104.

(55) Laerdahl, J. K.; Saue, T.; Faegri, K., Jr. *Theor. Chem. Acc.* **1997**, *97*, 177.

(56) Müller, B. G. *Angew. Chem., Int. Ed. Engl.* **1987**, *26*, 1081.

(57) Charpin, P.; Plurien, P.; Meriel, P. *Bull. Soc. Fr. Mineral. Cristallogr.* **1970**, *93*, 7.

(58) Fischer, P.; Schwarzenbach, D.; Rietveld, H. M. *J. Phys. Chem. Solids* **1971**, *32*, 543.

(59) Shen, C.; Zemva, B.; Lucier, G. M.; Graudejus, O.; Allman, J. A.; Bartlett, N. *Inorg. Chem.* **1999**, *38*, 4570.

(60) Elder, S. H.; Lucier, G. M.; Hollander, F. J.; Bartlett, N. *J. Am. Chem. Soc.* **1997**, *119*, 1020.

(61) Schröder, D.; Brown, R.; Schwerdtfeger, P.; Wang, X.-B.; Yang, X.; Wang, L.-S.; Schwartz, H. *Angew. Chem., Int. Ed.* **2003**, *42*, 311.

(50) Wells, A. F. *Structural Inorganic Chemistry*, 4th ed.; Clarendon Press: Oxford, 1975; p 349.

**Table 4.** Bond Lengths of Silver Monohalides (Distances in Angstrom, Angles in Degrees)

	method/basis set	F	Cl	Br	I	ref
AgX, $^1\Sigma_g, C_{\infty v}$	CCSD(T)/LB	1.988	2.297	2.385	2.551	this work
	experimental <sup>a</sup>	1.98318	2.28079	2.39311	2.54462	35–37
	see ref for details	1.987				55
	see ref for details	1.977				55
	see ref for details	2.01	2.31			51
	see ref for details	2.004				30
	CASSCF	1.99				52
	CASSCF		2.334			53
	CCSD(T)			2.42		21
	see ref for details			2.421		22
	CASSCF				2.655	54

<sup>a</sup> Experimental uncertainties are less than 0.000001 Å.

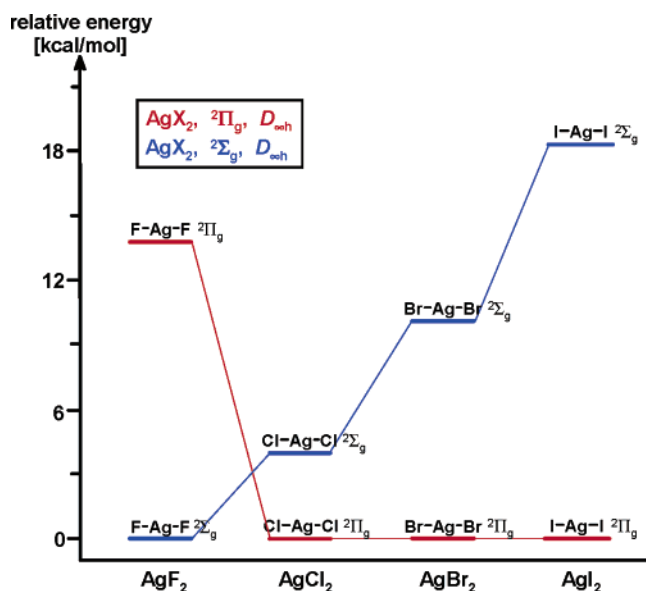


**Figure 6.** Relative energies of the  $^2\Sigma_g$  and  $^2\Pi_g$  state structures of  $\text{AgX}_2$  molecules from CCSD(T)/LB computations.

copper dihalides shows (vide infra), it is not yet clear what method and basis set can predict these values reliably.

There is one computational study of a silver dihalide,  $\text{AgBr}_2$ , in the literature by Rabilloud et al.<sup>21a</sup> Their conclusion is that the molecule has a  $C_{2v}$  symmetry structure, with a  $67^\circ$  bond angle and an Ag–Br bond distance of 2.699 Å. However, they only checked the  $C_{2v}$  symmetry arrangement and none of the linear ones, and there is no mention of a frequency analysis. Thus, there is no way of knowing what other structures they might have found had they not constrained the symmetry, or whether this  $C_{2v}$  symmetry structure is, indeed, a true minimum. We have also tried to calculate the  $C_{2v}$  symmetry structure, but it was impossible to get a proper and steady electronic state, as it often switched during optimization between  $^2A_1$  and  $^2B_2$ . Obviously, CASSCF calculations should be run for these molecules to get the proper electronic states, but that was beyond the scope of this study.

It is interesting to compare the structures of silver dihalides with those of the more stable copper dihalides. There is similarity in that for both systems, the difluorides have the  $^2\Sigma_g$  state as the ground state<sup>62</sup> and the  $^2\Pi_g$  state as the first excited state, while for the larger dihalides, the situation is the opposite.<sup>5,63</sup> For the much-studied copper dichloride (for refer-

ences, see ref 5), it has been found that its electronic states are very close to each other and that not only scalar relativistic effects but also spin–orbit effects have to be taken into account in the computation in order to get the right excitation energies. The computations agree in that, without taking spin–orbit effects into account, the ground state is the  $^2\Pi_g$  state, but the energy between the  $^2\Pi_g$  ground state and the  $^2\Sigma_g$  first excited state is calculated to be in a wide range, between about 200 and 6000  $\text{cm}^{-1}$ , depending on the method and basis set applied; a recent experimental value is about 1000  $\text{cm}^{-1}$ .<sup>63</sup> The latest study showed that if spin–orbit effects are taken into account, the ground state is a mixture of 59%  $^2\Pi_g$  and 41%  $^2\Sigma_g$ , lying about 330  $\text{cm}^{-1}$  below the  $^2\Pi_g$  state.<sup>5</sup> Apparently, this is an extremely difficult task for computations, especially if electronic excitations are to be calculated.

We might wonder why the  $^2\Sigma_g$  state is the ground state for the fluorides and the  $^2\Pi_g$  state for the other halides. The Wiberg bond indices show an interesting pattern. First, they are larger in the  $^2\Pi_g$  state molecules than in the  $^2\Sigma_g$  state molecules. That is, the Ag–X bonds of the  $^2\Pi_g$  state species are supposed to have a stronger covalent character. At the same time, the partial charges of the  $^2\Sigma_g$  state molecules are larger than they are for the  $^2\Pi_g$  state (Tables 2 and 3), and it seems that fluorine favors the  $^2\Sigma_g$  state as its ground state, with the larger ionic bonding character. The heavier  $\text{AgX}_2$  molecules favor the more covalently bound  $^2\Pi_g$  state.

The bond length of  $\text{AgF}_2$  is about the same in the two electronic states. For the larger dihalides, however, the Ag–X bond is significantly shorter in the  $^2\Pi_g$  state molecules. This can be explained by looking at their MOs. There is a  $\sigma$ -type bonding MO doubly occupied and a  $\pi$ -type antibonding MO singly occupied in the  $^2\Pi_g$  state. The occupancy of the same MOs is just the opposite in the  $^2\Sigma_g$  state molecules, where the bonding  $\sigma$  MO is singly and the antibonding  $\pi$  MO is doubly occupied; obviously a doubly occupied antibonding MO lengthens and possibly weakens a bond, which happens in the  $^2\Sigma_g$  state structures. The Wiberg indices (see Table 3) support this observation in that they indicate a larger degree of covalency for the Ag–X bonds in the  $^2\Pi_g$  than in the  $^2\Sigma_g$  molecules.

As mentioned above, the high-temperature disproportionated modification of silver difluoride,  $\text{Ag}[\text{AgF}_4]$ , is thermally unstable and undergoes an exothermic conversion to  $\text{AgF}_2$ . We also checked the reaction  $\text{Ag}[\text{AgX}_4] \rightarrow 2 \text{AgX}_2$  for the gaseous molecules for both the  $\Sigma$  and  $\Pi$  electronic states for all halides and found that they are all also exotherm with reaction energies

(62) Dyke, J. M.; Fayad, N. K.; Josland, G. D.; Morris, A. J. *Chem. Soc., Faraday Trans. 2* **1980**, *76*, 1672.

(63) Wang, X.-B.; Wang, L.-S.; Brown, R.; Schwerdtfeger, P.; Schroder, D.; Schwarz, H. *J. Chem. Phys.* **2001**, *114*, 7388.



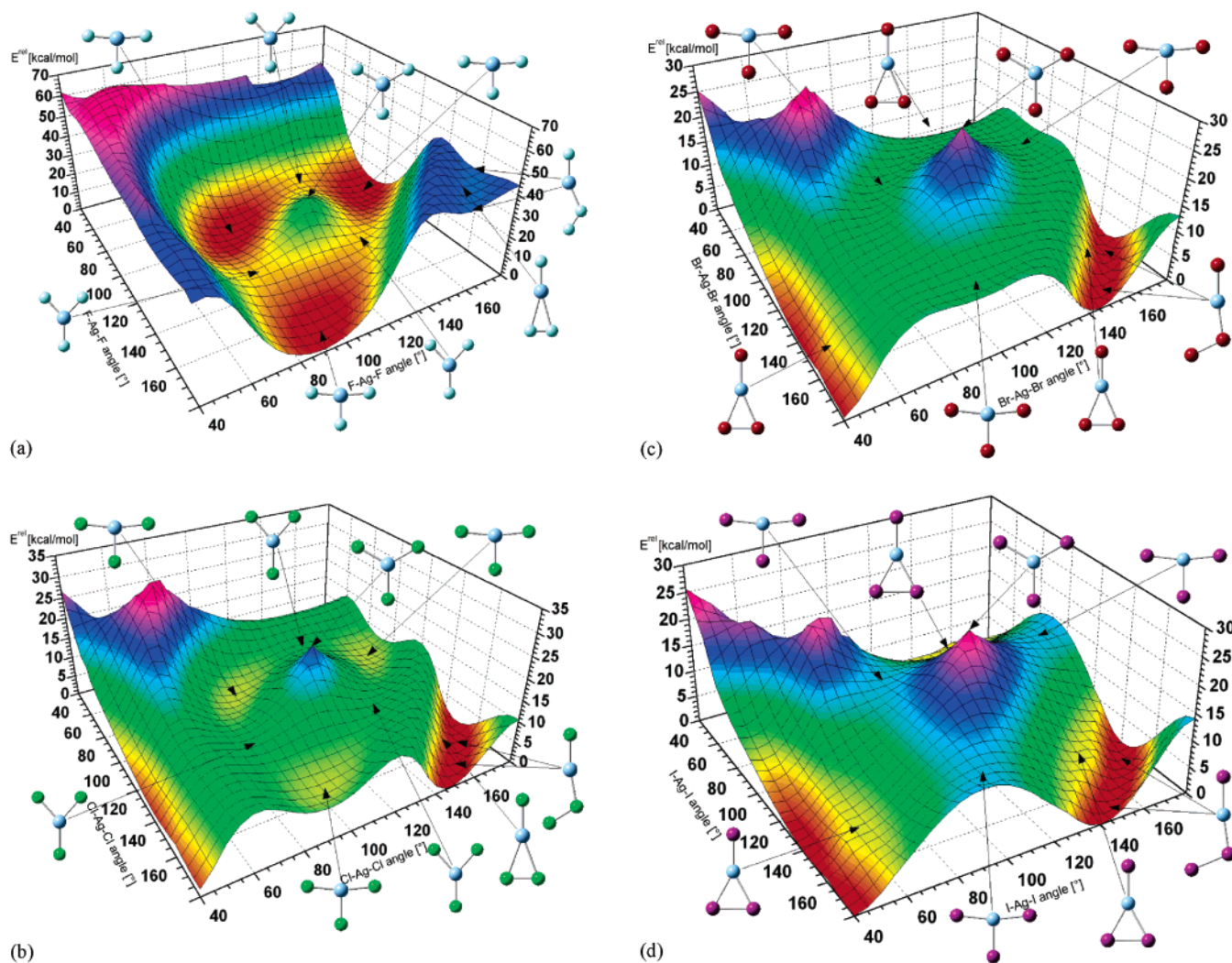


**Figure 7.** Potential energy surfaces of  $\text{AgX}_3$  molecules: (a)  $\text{AgF}_3$ , (b)  $\text{AgCl}_3$ , (c)  $\text{AgBr}_3$ , and (d)  $\text{AgI}_3$ . Note the different energy scales.

of  $-93$  kcal/mol for the  $\Sigma$  state of  $\text{AgF}_2$  and well below  $-100$  kcal/mol for the  $\Pi$  state of the other dihalides at the B3LYP/LB level (see Table S30 in the Supporting Information).

One more comment is worthwhile concerning the structure of isolated  $\text{AgX}_2$  molecules. Their crystals have a low-symmetry tetragonally distorted structure due to the Jahn–Teller effect (vide supra). As is well-known, however, linear molecules are special cases, for which the Jahn–Teller distortion does not apply,<sup>31</sup> and this is why they have a high-symmetry linear structure.

**Silver Trihalides.** The only known silver trihalide is  $\text{AgF}_3$ , and it is one of the most powerful oxidizing agents.<sup>8</sup> It was found thermodynamically unstable and isostructural with  $\text{AuF}_3$  in its crystal. Both  $\text{AuF}_3$  and  $\text{AgF}_3$  consist of helical chains, in which square-planar  $\text{MF}_4$  units are connected via *cis*-fluorine atoms.<sup>8,64</sup> As Bartlett et al.<sup>8</sup> comments, the two structures are almost isodimensional as their bond lengths differ only in the thousandths of an angstrom. This similarity appears in their gas-phase geometries, as well, in that their bond angles are practically identical and one of their bond lengths is also the same.

Earlier, it was found both by experiment<sup>32</sup> and computations<sup>6,32,33</sup> that gold trihalides are subject to Jahn–Teller distortions, and this could be expected for the silver trihalides, as well. Indeed, as the PESs of the  $\text{AgX}_3$  molecules show (see Figure 7), the  $D_{3h}$  symmetry structure is not a minimum energy structure for either of the silver trihalides. The four PESs show a gradually changing pattern.  $\text{AgF}_3$  is very similar to  $\text{AuF}_3$ ,<sup>6,32</sup> It has a typical Mexican-hat PES around the  $D_{3h}$  symmetry geometry (see Figure 7a); there are three distinct minima along the brim of the hat with three saddle points between them, indicative of Jahn–Teller distortions for which the quadratic coupling terms are of importance in describing the vibronic interaction.<sup>65</sup> The structure corresponding to the minima has a T-shape, and the one corresponding to the saddle points, describing the transition state between two minima by way of exchanging the positions of the X2 and X3 or X4 atoms, has a Y-shape, just as in case of  $\text{AuF}_3$ . The energy difference between these two structures is about 10 (CCSD(T)) [9 (B3LYP)] kcal/mol,<sup>66</sup> so the molecule can be considered as a static JT system. The energy differences of the different  $\text{AgX}_3$  isomers are shown

(64) Einstein, F. W. B.; Rao, P. R.; Trotter, J.; Bartlett, N. *J. Chem. Soc. A* **1967**, 478.

(65) Bersuker, I. A. *Electronic Structure and Properties of Transition Metal Compounds*; John Wiley & Sons: New York, 1996.

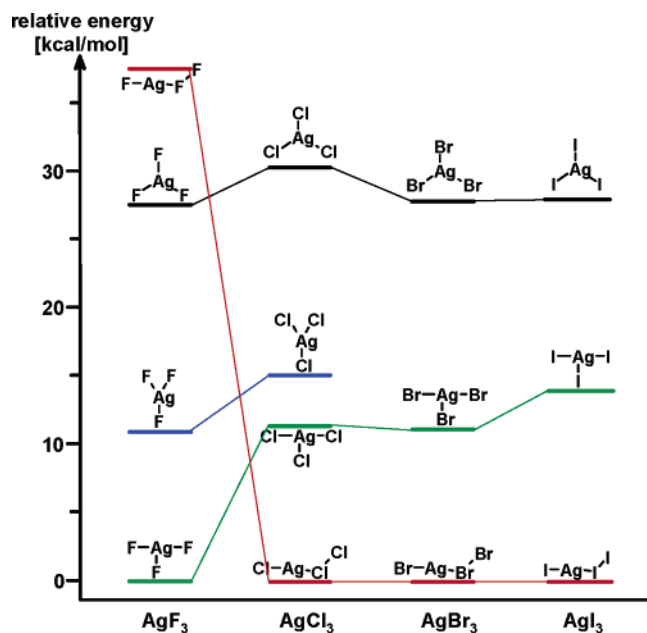


**Figure 8.** Energy differences between different  $\text{AgX}_3$  isomers from CCSD(T)/LB calculations.

in Figure 8. The T-shape structure of  $\text{AgF}_3$  lies about 27 [26] kcal/mol lower than the undistorted  $D_{3h}$  symmetry structure.

We have checked the PES outside the JT surface, but all other structures are much higher in energy; so the T-shape structure is the global minimum for this molecule by each method. For the other three trihalides, however, this is no longer the case. For  $\text{AgCl}_3$ , we still have a Mexican-hat JT surface, and within this surface, the T-shape structure is still lower in energy than the Y-shaped, but only by about 4 [3] kcal/mol. At the same time, there is an L-shape structure (see Figure 1) outside the JT surface, which is 10 [6] kcal/mol lower in energy than the T-shaped structure and is the global minimum for  $\text{AgCl}_3$  (see Figures 7b and 8). This L-shape structure also appears on the PES of  $\text{AgF}_3$ , and it is a stable structure but it is about 38 [30] kcal/mol higher in energy than the T-shape global minimum. For  $\text{AgBr}_3$  and  $\text{AgI}_3$ , the potential energy surface around the  $D_{3h}$  symmetry structure starts to lose the Mexican-hat character. It not only becomes flat but also continues down outside this surface without any energy barrier toward the L-shape structure. The computations could not locate a Y-shape structure but a loose  $C_{2v}$  symmetric  $\text{AgX}\cdot\text{X}_2$  complex (notation:  $\text{TS}-\text{AgX}\cdot\text{X}_2$ ) outside the JT surface (Figure 7c,d) with rather long bonds between the two fragments. This loose complex represents a transition state for  $\text{AgBr}_3$  and  $\text{AgI}_3$  (one negative frequency, see later in the discussion of the L-shape structure). The reason is that for  $\text{AgBr}_3$  and  $\text{AgI}_3$ , the shape of the PES is dominated by the deep energy valley of the L-shape isomer; hence, all attempts to localize a Y-shape isomer for  $\text{AgBr}_3$  and  $\text{AgI}_3$  failed.

The geometrical parameters of the different isomers of  $\text{AgX}_3$  molecules are given in Table 1. The T-shape isomer has two smaller and one larger  $\text{X}-\text{Ag}-\text{X}$  bond angles as also shown in Figure 1. The angular distortion from the  $D_{3h}$  symmetry trigonal planar arrangement is rather large. It was observed earlier that relativistic effects enhanced the Jahn–Teller distur-

tions in all  $\text{AuX}_3$  molecules by lowering the energy of the Au 6s orbital and by increasing the energy of the 5d orbital.<sup>6</sup> Similar phenomenon has been found for the silver trihalides. For these molecules, the energies of the 4d and 5s orbitals become comparable, and the 4d orbitals become major contributors to the valence shell and their shape favors a large angular distortion. The angular distortion in silver trihalides is about as large as that in the gold trihalides. The partial charges from a natural bond orbital (NBO) analysis for both the T- and Y-shape isomers are given in Table 2.  $\text{AgF}_3$  is a highly polarized molecule, in which the halogen charge is somewhat smaller on the X2 atom than on the X3,4 atoms for the T-shape structure and vice versa for the Y-shape structure. The charges as well as the polarization decrease from the trifluoride to the triiodide.

The Wiberg bond index is largest for the T-shape  $\text{AgF}_3$  molecule among all systems, in agreement with the general observation that the covalent character is larger; the higher is the formal oxidation number of the metal.

There is a considerable  $\pi$  back-bonding in the T-shape structures of these molecules. Figure 9 shows some of the  $\pi$  MOs, with  $b_1$ ,  $a_2$  (both out-of-plane), and  $b_2$  (in-plane) symmetry. The  $a_2$  MO is a three-center bond, whereas the  $b_2$  MO is delocalized over the entire molecule. The  $\pi$  bonding decreases gradually from  $\text{AgF}_3$  to  $\text{AgBr}_3$ ; in  $\text{AgI}_3$ , there is no  $\pi$  overlap.

For three out of the four silver trihalides, the L-shape structure is the global minimum. This structure is considerably lower in energy than any of the other possible structures for the three heavier trihalides (see Figures 7 and 8). It is more stable than the T isomer by 11, 11, and 14 kcal/mol at the CCSD(T)/LB level (6, 11, and 13 kcal/mol at the B3LYP/SB level, corresponding to Figure 7), for the chloride, bromide, and iodide, respectively. This L-shape isomer has  $C_s$  symmetry, as shown in Figure 1. It has only two metal–halogen bonds and one direct  $\text{X}-\text{X}$  interaction. The two metal–halogen bonds are quite different. The  $\text{Ag}-\text{X}_2$  bond is about 0.10 Å longer than the corresponding bond in the T-shape isomer for  $\text{AgF}_3$ . For the other three trihalides, this difference gradually decreases to 0.07 and 0.01 Å, and finally, for  $\text{AgI}_3$ , the bond is 0.01 Å shorter than the same bond in the T-shape isomer. This trend corresponds to the relative stabilities of these isomers in the different trihalides. The  $\text{Ag}-\text{X}_2$  bond is about the same length as the bond in the monohalide, within 0.01 Å. The covalent bond order of this bond is in accord with this; it increases from the fluoride toward the iodide and is somewhat smaller than the bond order of the monohalide molecules (see Table 3). The NBO charges (see Table 2) indicate that the  $\text{Ag}-\text{X}_2$  bond is highly polar with a considerable ionic character, only slightly less so than the bonds in the monohalide molecules; the trend decreases toward the iodides as expected.

The  $\text{Ag}-\text{X}_3$  bond is longer than  $\text{Ag}-\text{X}_2$ , by about 0.4 Å for  $\text{AgF}_3$  and about 0.1–0.2 Å for the other three trihalides. The difference corresponds to the fact that for  $\text{AgF}_3$ , this structure is a high-energy configuration, while for the other three molecules, it is the global minimum. It is no surprise that for  $\text{AgF}_3$ , the T-shape “real” trihalide is more stable, as fluorine stabilizes high-oxidation states (vide supra). The bond orders increase toward the heavier trihalides. The  $\text{Ag}-\text{X}_3$  bond length in the L-shape silver trifluoride is 2.410 Å, which is hardly a bond; its covalent bond order is very small (0.07). This is in accord with the high energy of this molecule; it is hardly

(66) As noted before, our discussion is based on the CCSD(T) results. At the same time, since the PESs were calculated by the B3LYP method, the B3LYP values will also be given in brackets after the CCSD(T) energy value. The values given in brackets are relevant to Figure 7.

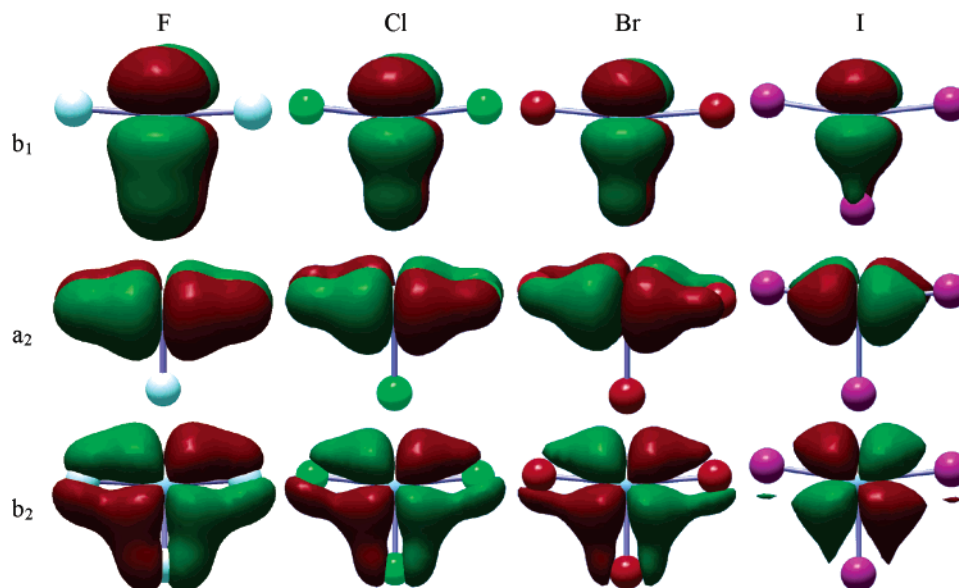


**Figure 9.** Molecular orbitals showing in-plane and out-of-plane  $\pi$ -type bonding in the T-shape isomer of  $\text{AgX}_3$  molecules (HF orbitals at CCSD(T)/LB geometries).

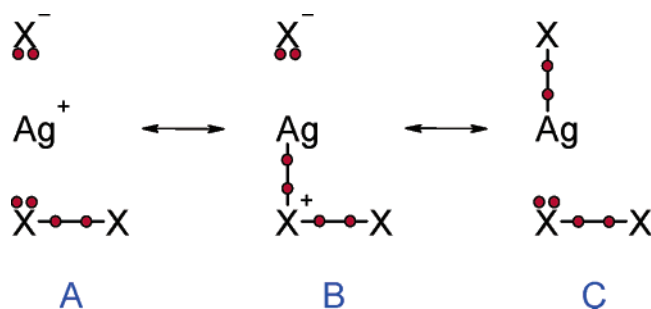


**Figure 10.** Different Lewis representations of the L-shape silver trihalides.

different from an ensemble of separate  $\text{AgF}$  and  $\text{F}_2$  molecules. The  $\text{Ag}-\text{X}_3$  bond in the other three trihalides is more realistic, but it still is a weak bond, with its covalent bond orders being about one-third of the bond order of the  $\text{Ag}-\text{X}_2$  bond. The third bond of the trihalide,  $\text{Ag}-\text{X}_4$ , however, is no longer a bond in this isomer; it is more than 1 Å longer than the  $\text{Ag}-\text{X}_2$  bond in all silver trihalides. Finally, there is a new bond here,  $\text{X}_3-\text{X}_4$ , which is only about 0.01 Å longer in all four molecules than the bond in the free halogen molecules. Accordingly, its covalent bond order is close to 1.

On the PES of all silver trihalides (Figure 7), there are two L-shape structures with equal energy, depending on which of the two halogen atoms of the  $\text{X}_2$  molecule the silver atom is attached to. These two L-shape minima are separated by a small energy barrier (F, 5.4; Cl, 5.4; Br, 5.9; and I, 4.7 kcal/mol), which is associated with a transition state. This transition state corresponds to the  $C_{2v}$  symmetric  $\text{TS}-\text{AgX}\cdot\text{X}_2$  structure described above, which is a loose complex of the  $\text{AgX}$  and  $\text{X}_2$  molecules.

We already found a similar L-shape structure for  $\text{AuI}_3$  earlier<sup>6</sup> and rationalized it with VB considerations. The same reasoning applies for these silver halides, as well. Figure 10 shows three possible canonical Lewis structures (A–C). In these structures, those lone electron pairs that do not participate in the bond are omitted. The NBO analysis is based on localized two-center bonds and lone pairs. It considers only one  $\sigma$  bond between Ag and  $\text{X}_2$  and one  $\sigma$  bond between  $\text{X}_3$  and  $\text{X}_4$ ; this corresponds

**Table 5.** Donor–Acceptor Interactions (kcal/mol),<sup>a</sup> Charge Transfer ( $q_{\text{ct}}$  in e),<sup>a</sup> and Orbital Energies (au)<sup>b</sup> in the L-Shape  $\text{AgX}_3$  (X = F, Cl, Br, I) Molecules

	F	Cl	Br	I
donor–acceptor interaction				
$\Sigma E^{(2)} [\text{AgX} \rightarrow \text{X}_2]$	1.60	4.19	7.87	7.41
$\Sigma E^{(2)} [\text{X}_2 \rightarrow \text{AgX}]$	10.38	37.31	47.48	55.19
sum $E^{(2)}$	11.98	41.50	55.35	62.60
$E^{(2)} [p_x\text{-LP}(\text{X}_3) \rightarrow \sigma^*(\text{AgX})]$	6.70	24.62	32.09	39.07
charge transfer				
$q_{\text{ct}} (\text{X}_2 \rightarrow \text{AgX})$	−0.03500	0.03814	0.04907	0.07388
HOMO–LUMO gap				
HOMO( $\text{X}_2$ ), ( $\pi_g$ )	−0.66990	−0.44652	−0.40543	−0.35964
LUMO( $\text{AgX}$ ), ( $\sigma_v^*$ )	−0.02193	−0.02392	−0.02216	−0.02241
$\Delta[\text{HOMO}–\text{LUMO}]$	0.64797	0.42260	0.38327	0.33723

<sup>a</sup> B3LYP/SB level at the CCSD(T)/LB geometry. <sup>b</sup> Orbital energies at the CCSD(T) level.

to structure C in Figure 10. In this structure, the molecule consists of two separate, closed-shell fragments,  $\text{AgX}$  and  $\text{X}_2$ . The partial charges calculated for the L-isomer support such a description of the structure.

As Tables 2 and 3 indicate, the partial charges on the Ag and  $\text{X}_2$  atoms are only slightly smaller than those of the monohalides, while those of the other two atoms,  $\text{X}_3$  and  $\text{X}_4$  are close to zero. This indicates that Lewis structure C is the best description of this isomer. The slightly positive charges on  $\text{X}_3$  of  $\text{AgX}\cdot\text{X}_2$  (X = Cl, Br, I) arise from the resonance with structure B of Figure 10. Structure A in this figure represents an ionic structure, which considering the high partial charges on the Ag and  $\text{X}_2$  atoms (decreasing from 0.83 to 0.49 on Ag and from −0.79 to −0.56e on  $\text{X}_2$  from the fluoride toward the iodide, respectively), seems to play an important role, as well.

On this basis, the L-shape isomer can be considered as a donor–acceptor molecule. We have looked into the intramolecular donor–acceptor interaction between the two closed-shell fragments. We found an appreciable interaction between the p-type lone pair of  $\text{X}_3$  of the  $\text{X}_2$  unit with the antibonding  $\sigma$  orbital ( $\sigma^*$ ) of the  $\text{AgX}$  unit for all species (see Table 5). We have calculated the energy associated with this resonance by a second-order perturbation approach. It is rather small for the



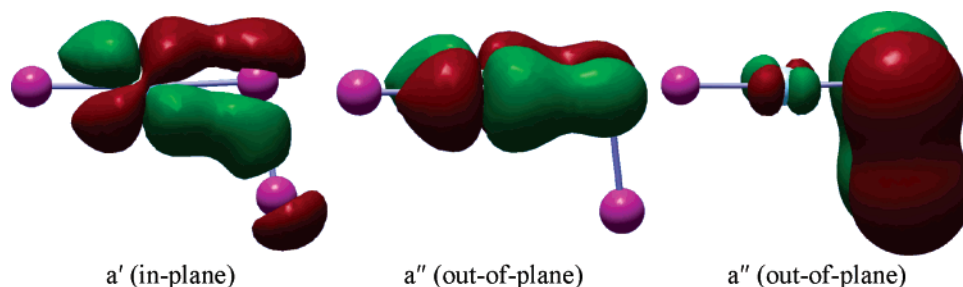


**Figure 11.** Some  $\pi$ -type molecular orbitals for the L-shape  $\text{AgI}_3$  molecule (HF orbitals at CCSD(T)/LB geometry).

fluoride, about 7 kcal/mol, and it is increasing toward the iodide: 25, 32, and 39 kcal/mol for  $\text{AgCl}\cdot\text{Cl}_2$ ,  $\text{AgBr}\cdot\text{Br}_2$ , and  $\text{AgI}\cdot\text{I}_2$ , respectively.

It was also interesting to find that mostly the  $\text{X}_2$  fragment acts as the donor and the  $\text{AgX}$  fragment as the acceptor. The overall charge transfer from the  $\text{X}_2$  unit to the  $\text{AgX}$  unit increases from the fluoride toward the iodide (see Table 5). In this interaction, the HOMO of  $\text{X}_2$  is a  $\pi_g$  MO, corresponding to the lone electron pairs, and the LUMO of  $\text{AgX}$  is an antibonding  $\sigma_g^*$  molecular orbital. The HOMO–LUMO gap is largest for the  $\text{AgF}\cdot\text{F}_2$  adduct, and it decreases toward the  $\text{AgI}\cdot\text{I}_2$  system. Of course, it is not only the HOMO–LUMO interactions that contribute to this Lewis acid–base interaction. As Figure 11 indicates for  $\text{AgI}_3$ , there are different interactions between the two parts of this donor–acceptor system.

The L-shape isomer of  $\text{AgX}_3$ , with its donor–acceptor interaction between  $\text{AgX}$  and  $\text{X}_2$ , is one type of the so-called closed-shell interactions, which have recently received a great deal of attention.<sup>27,28</sup> These interactions encompass all intermolecular interactions, such as hydrogen bonding, donor–acceptor or charge-transfer bonding, metallophilic interactions, and any other attractive interactions between atoms and molecules.

$\text{X}_3^-$  ions are known for all halogens; therefore, we also checked if a structure consisting of  $\text{Ag}^+$  and  $\text{X}_3^-$  ions would not be stable. We tested different geometrical arrangements for this type of “trihalide”, but all of these structures are unstable and disproportionate to  $\text{AgX}$  and  $\text{X}_2$ .

**Bonding in Silver Halides.** The calculated Wiberg bond indices are given in Table 3. For the minimum-energy structures of the  $\text{Ag}_2\text{X}$  ( $C_{2v}$  geometries),  $\text{AgX}$ , the  ${}^2\Pi_g$  state  $\text{AgX}_2$ , and the L-shape  $\text{AgX}_3$  ( $\text{X} = \text{Cl}, \text{Br}, \text{I}$ ) molecules, our computations show an increase of covalency of the  $\text{Ag}-\text{X}$  bond, the heavier the halogen, as indicated by the calculated Wiberg bond indices (WBI).<sup>46</sup> The partial charges are in agreement with this.

Earlier, we mentioned that for the  $\text{AgX}_2$  molecules, the Wiberg indices are larger for the  ${}^2\Pi_g$  state than for the  ${}^2\Sigma_g$  state molecules, and this must be at least one of the reasons why the  ${}^2\Pi_g$  state structures are the ground state structures for the larger dihalides.

We carried out AIM analyses on all silver halide molecules. Every expected bond critical point (3,−1)<sup>67</sup> was found in all molecules and characterized by its Laplacian at the bond CP (see Supporting Information). In addition to the expected bond path network (3,−1), bond CPs were found on the  $\text{Ag}\cdots\text{Ag}$  lines in  $\text{Ag}_2\text{X}$ , describing a covalent  $\text{Ag}-\text{Ag}$  interaction (Figure 12). A ring CP inside the  $\text{Ag}-\text{X}-\text{Ag}$  space was also found, thus

the Poincaré–Hopf rule<sup>68</sup> is satisfied, and according to Bader, this is a good indication of bonding between these atoms.<sup>69</sup>

For all silver halides (for all CPs describing the  $\text{Ag}-\text{X}$  and  $\text{Ag}-\text{Ag}$  bonds), small values of  $\rho(\mathbf{r}_b)$  and positive values of  $\nabla^2\rho(\mathbf{r}_b)$  were found (see Supporting Information). This would indicate “closed-shell interactions” rather than “shared interaction” according to the original formulation.<sup>47</sup> At the same time, small negative values were found for the total electronic energy density,  $H(\mathbf{r}_b)$  (except for  $\text{Ag}_2\text{F}$  and  $\text{AgF}$ ), which would indicate covalent bonding.<sup>70</sup> Small values of  $\rho(\mathbf{r}_b)$  and  $\nabla^2\rho(\mathbf{r}_b)$  for the  $\text{Ag}-\text{Ag}$  and  $\text{Ag}-\text{X}$  bonds have often been found in transition-metal compounds containing metal–metal and metal–nonmetal bonds,<sup>71,72</sup> and they do not necessarily indicate weak chemical bonds. The topological properties of covalent bonds involving transition metals do not have the same characteristics as covalent bonds between first-row atoms. Experimental studies on transition-metal complexes displayed almost invariably a positive Laplacian for any bonds involving the transition metal.<sup>72,73</sup>

Macchi and Sironi,<sup>72</sup> in a recent review of charge density studies on transition metal carbonyl compounds, argued that these bonds, characterized by relatively low  $\rho(\mathbf{r}_b)$ ,  $G(\mathbf{r}_b)$ , and  $|V(\mathbf{r}_b)|$  values a positive  $\nabla^2\rho(\mathbf{r}_b)$  value and negative  $H(\mathbf{r}_b)$ , should be considered as open-shell (covalent) interactions. Since the total energy density is negative for the  $\text{Ag}-\text{Ag}$  bond in the  $C_{2v}$  symmetry  $\text{Ag}_2\text{X}$  systems, albeit marginally so, that bond might be classified as a covalent bond (open-shell), rather than metallic or closed-shell (small  $\rho(\mathbf{r}_b)$ , small positive values of  $\nabla^2\rho(\mathbf{r}_b)$ ,  $G(\mathbf{r}_b)/\rho(\mathbf{r}_b) < 1$ ,  $H(\mathbf{r}_b)/\rho(\mathbf{r}_b) < 0$ ).<sup>72</sup> This is in agreement with the NBO analysis. The classification of the  $\text{Ag}-\text{X}$  bonds is more difficult. For  $\text{Ag}_2\text{F}$ , the  $\text{Ag}-\text{F}$  bond can be regarded as ionic since positive values were found for the total electronic energy density in addition to the positive values of  $\nabla^2\rho(\mathbf{r}_b)$ . The total electronic energy density is also positive for  $\text{AgF}$ , but only marginally (0.0004). For the other  $\text{Ag}/\text{X}$  species, small negative values were found for  $H(\mathbf{r}_b)$  beside a small positive Laplacian. These positive values should not be taken as indicative of pure closed-shell (ionic) interaction between the  $\text{Ag}$  and  $\text{X}$  atoms. Following Macchi’s and Sironi’s<sup>72</sup> suggestion, we could classify the  $\text{Ag}-\text{X}$  bond as intermediate between ionic and covalent

(67) For nomenclature definitions of critical points, see ref 47.

(68) Bader, R. F. W. *Chem. Rev.* **1991**, *91*, 893–928.

(69) Bader, R. F. W. *J. Phys. Chem. A* **1998**, *102*, 7314–7323.

(70) (a) Cremer, D.; Kraka, E. *Angew. Chem.* **1984**, *96*, 612; *Angew. Chem., Int. Ed. Engl.* **1984**, *23*, 62. (b) Closed-shell interactions are dominated by the kinetic energy density,  $G(\mathbf{r}_b)$ , in the region of the bond CP, with  $G(\mathbf{r}_b)$  being slightly greater than the potential energy density  $|V(\mathbf{r}_b)|$  and the energy density  $H(\mathbf{r}_b) > 0$  close to zero.

(71) Farrugia, L. J.; Mallinson, P. R.; Stewart, B. *Acta Crystallogr.* **2003**, *B59*, 234–247.

(72) Macchi, P.; Sironi, A. *Coord. Chem. Rev.* **2003**, *238–239*, 383–412 and references therein.

(73) Frenking, G.; Fröhlich, N. *Chem. Rev.* **2000**, *100*, 717–774.



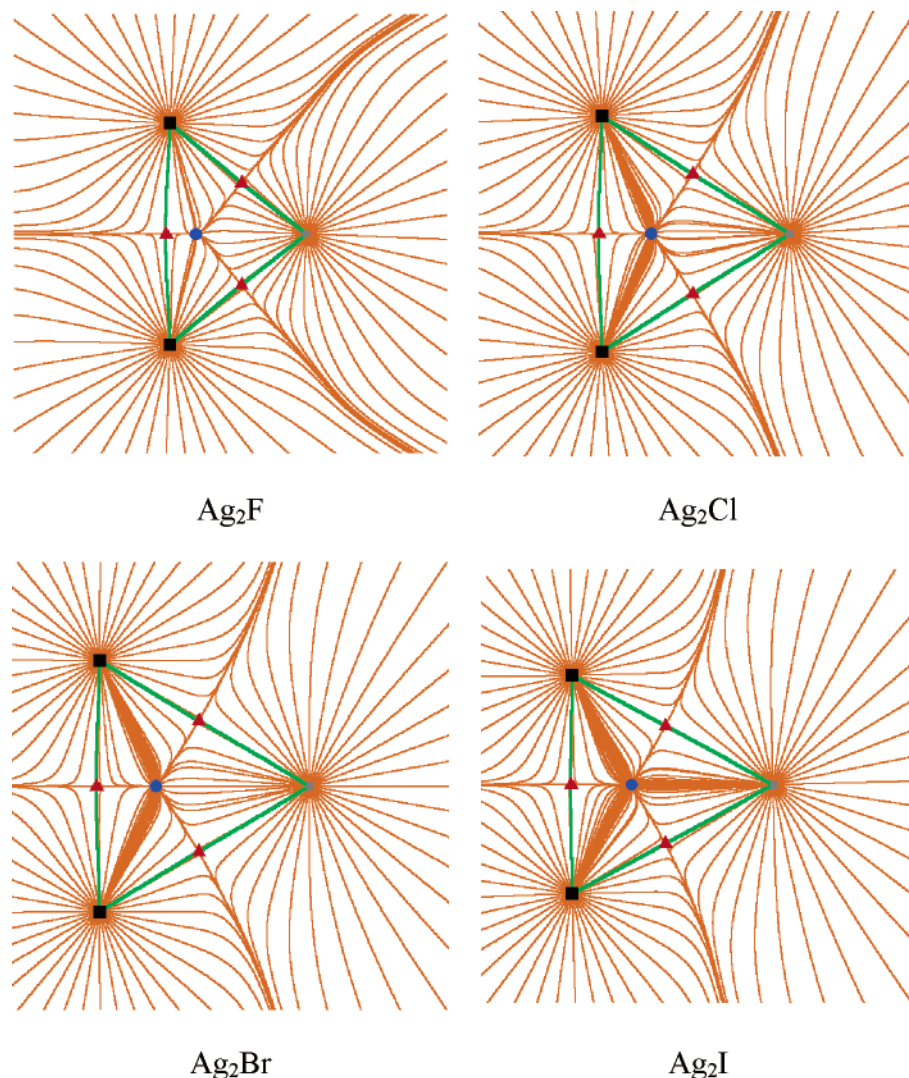


**Figure 12.** Gradient lines of the electron density in  $\text{Ag}_2\text{X}$  molecules and the projection of the molecular graph onto the  $\text{Ag}-\text{Ag}-\text{X}$  plane. The bond CPs are shown as red triangles, the ring CPs as blue circles, the two Ag atoms as black, and the halogen as gray rectangle.

(small  $\rho(\mathbf{r}_b)$ , small positive values of  $\nabla^2\rho(\mathbf{r}_b)$ ,  $G(\mathbf{r}_b)/\rho(\mathbf{r}_b) \sim 1$ ,  $H(\mathbf{r}_b)/\rho(\mathbf{r}_b) < 0$ ).

## Conclusions

There is a great diversity among the structures of the halides of the coinage metals. The metal atom can appear in different oxidation states, and the stability of different oxidation states is rather different among them. For example, while the +1 oxidation state is most stable for the silver halides, for copper, the most stable is the +2 oxidation state. Silver, as the second element in this group, has perhaps the richest diversity of its halides, from the  $\text{Ag}_2\text{X}$  subhalide to the trihalide and many versions of mixed halides in the solid state.

The most common silver halide is the monohalide; all four of them are well-known. The other valencies, on the other hand, are mostly confined to the fluorides. This is not so surprising as it is well-known that fluorine stabilizes larger oxidation states of metals. Relativistic effects also play a role in stabilizing larger oxidation states. This is why, although for silver the +3 oxidation state is probably the highest reachable, for gold, the +5 is also known, and according to Neil Bartlett,<sup>74</sup> even the electrochemical generation of  $\text{AuF}_6$  might happen some day.

Silver subfluoride,  $\text{Ag}_2\text{F}$ , is a well-known compound. Our computations showed that the other subhalides are also thermodynamically stable structures. The situation is different for the silver dihalides. There, again, silver difluoride ( $\text{AgF}_2$ ) is a well-known compound. The disproportionation reaction  $2 \text{AgX}_2 \rightarrow \text{AgX} + \text{AgX}_3$  appears to be endothermic for  $\text{AgF}_2$ , in line with the fact that  $\text{AgF}_2$  is a known compound (see Supporting Information). For the other three silver dihalides, this reaction is exothermic. Taking always the minimum energy structures into consideration (i.e.,  ${}^2\Sigma_g$  for  $\text{AgF}_2$  and  ${}^2\Pi_g$  for the rest of the dihalides and T-shape  $\text{AgF}_3$  and L-shape  $\text{AgX}_3$  for the rest of the trihalides), the CCSD(T)/LB energies of the above reaction are 14.9, -14.9, -13.5, and -13.9 kcal/mol for the fluorides, chlorides, bromides, and iodides, respectively (the corresponding  $\Delta G_{298}$  values at the CCSD(T)/SB level are 17, -14, -15, and -13 kcal/mol, respectively). Thus, the larger silver dihalides do not seem to be thermodynamically stable enough to be prepared in the vapor phase as isolated molecules unless they are kinetically stable.

The second ionization potential of silver is larger than that of gold, showing that the 4d electrons of silver are much more

(74) Bartlett, N. *Gold Bull.* **1998**, *31*, 22.

strongly bound than the 5d electrons of gold, due to the larger destabilizing of 5d electrons by relativistic effects. As Hoffmann<sup>7</sup> puts it, “Ag(II), Ag(III) and F are all about equally hungry for electrons”. This is also the reason AgF<sub>2</sub> is such a strong oxidizing agent. However, the larger oxidation state of silver is only stabilized by the electronegative fluorine atom, and the larger halogens cannot provide a strong enough bond.

Finally, consider the silver trihalides. We checked two types of decomposition reactions for AgX<sub>3</sub>, AgX<sub>3</sub> → AgX<sub>2</sub> + 1/2 X<sub>2</sub>, and AgX<sub>3</sub> → AgX + X<sub>2</sub>. For the T isomer of AgF<sub>3</sub>, both reactions are estimated to be endothermic at all levels of theory ( $\Delta E_0$  is 14 and 43 at the CCSD(T)/LB, and  $\Delta G_{298}$  is 6 and 30 kcal/mol at the CCSD(T)/SB level for the two reactions above, respectively). Thus, we can say that according to our results, the T-shape AgF<sub>3</sub> molecule is intrinsically stable in the gas phase. Bartlett et al.’s earlier comments on this molecule<sup>8</sup> being thermodynamically unstable refer to the practical situation when the presence of even a very small amount of fluorine and its reactions with the environment (even the wall of a quartz container or the reaction of AgF<sub>3</sub> with traces of water) may catalyze the decomposition. We also looked at the decomposition of the other silver trihalides, AgX<sub>3</sub> (X = Cl, Br, I). For their T-shape isomer, the decomposition is spontaneous, in agreement with the fact that the T isomer is the global minimum only for AgF<sub>3</sub>. The situation is the opposite for the L isomer, which is the global minimum for AgCl<sub>3</sub>, AgBr<sub>3</sub>, and AgI<sub>3</sub>. The decomposition of the L isomer of AgF<sub>3</sub> (a high-energy local minimum on the PES) is spontaneous. Decomposition of the

other three silver trihalides, on the other hand, is endothermic and increasingly so from the trichloride ( $\Delta H_{298} = 9$ ;  $\Delta G_{298} = 2$  kcal/mol) toward the triiodide ( $\Delta H_{298} = 14$ ;  $\Delta G_{298} = 7$  kcal/mol), indicating an increasing stability for the L-shape isomer from AgF<sub>3</sub> to AgI<sub>3</sub>. This thermodynamic stability of their gas-phase molecules does not necessarily mean that these molecules can be prepared. Much would depend on lattice energies that may or may not favor the adduct formation and on reaction kinetics. Of course, we have to remember that in this L-shape isomer the metal is not in its formal +3 oxidation state, rather, these molecules are loose complexes of AgX and the X<sub>2</sub> molecule.

**Acknowledgment.** We are indebted to the Leibniz Rechenzentrum Munich for help and a generous allocation of CPU time, and to the Hungarian Scientific Research Fund for support (Grant No. OTKA T 037978).

**Supporting Information Available:** Computational details, bond lengths of all silver halides, Ag<sub>2</sub>, Ag<sub>2</sub><sup>+</sup>, and X<sub>2</sub> molecules (X = F, Cl, Br, I) at all computational levels; harmonic vibrational frequencies, relative energies for all silver halides at different computation levels, reaction energies, ionization energies for Ag and Ag<sub>2</sub>, results of the AIM analysis. This material is available free of charge via the Internet at <http://pubs.acs.org>.

JA051442J